Weak Lensing Detection in CMB Maps

F. Bernardeau

Service de Physique Théorique, C.E. de Saclay, F-91191 Gif-sur-Yvette cedex, France

June 13, 2018

arXiv:astro-ph/9611012v2 5 Mar 1997

Abstract. The weak lensing effects are known to change only weakly the shape of the power spectrum of the Cosmic Microwave Background (CMB) temperature fluctuations. I show here that they nonetheless induce specific non-Gaussian effects that can be detectable with the *four-point correlation function* of the CMB anisotropies. The magnitude and geometrical dependences of this correlation function are investigated in detail. It is thus found to scale as the square of the derivative of the two-point correlation function and as the angular correlation function of the gravitational displacement field. It also contains specific dependences on the shape of the quadrangle formed by the four directions.

When averaged at a given scale, the four-point function, that identifies with the connected part of the fourth moment of the probability distribution function of the local filtered temperature, scales as the square of logarithmic slope of its second moment, and as the variance of the gravitational magnification at the same angular scale.

All these effects have been computed for specific cosmological models. It is worth noting that, as the amplitude of the gravitational lens effects has a specific dependence on the cosmological parameters, the detection of the four-point correlation function could provide precious complementary constraints to those brought by the temperature power spectrum.

Key words: Cosmology: Dark Matter, Large-Scale Structures, Gravitational Lensing, Cosmic Microwave Background

1. Introduction

A robust prediction of inflationary scenarios is that the temperature fluctuations of the Cosmic Microwave Background (CMB) are expected to obey Gaussian statistics. Actually this prediction has been challenged recently by

Send offprint requests to: F. Bernardeau; fbernardeau@cea.fr

several authors (Falk, Rangarajan & Srednicki 1993, Munshi, Souradeep & Starobinsky 1995) who calculated the skewness induced by nonlinear couplings in the primary[1] stage of the temperature fluctuation generation. The skewness induced at this level has been found, however, to be entirely negligible compared to the cosmic variance, and thus not accessible to detections. Therefore, the primary temperature maps are entirely defined, in a statistical sense, by the power spectrum of the temperature fluctuations or equivalently by the shape of the two-point correlation function. A number of other statistical indicators are thus set up by this a priori hypothesis. In particular Bond & Efstathiou (1987) have investigated expected properties of such temperature maps, as the number density of temperature peaks, their correlation functions... Moreover, the exploration of the CMB physics has been boosted recently after it has been realized that it would be possible to determine all the cosmological parameters with a remarkable precision from an accurate, and accessible, measurement of the temperature power spectrum (Jungman et al. 1996). In particular, the effects of the secondary sources of temperature fluctuations (Sunyaev-Zel'dovich effects, nonlinear Doppler effects, lenses..) and foregrounds (point sources, galactic dust) on the power spectrum have been investigated in more details (see Cobras/Samba report, 1996, for a general discussion on these problems). These calculations have shown that most, if not all, of these effects have a relatively small impact on it. In these calculations, however, the impact of secondary effects on the Gaussian nature of the temperature field has not been considered. Particularly interesting are the the higher order correlation functions that are identically zero for Gaussian fields, and are thus direct indicators of any, even small, non-Gaussian features.

In this paper the calculations will be focused on the effects of weak-lensing on CMB maps. They, indeed, constitute a particularly attractive mechanism because it comes

---

[1] "primary" means the anisotropies induced on the last scattering surface by either potential fluctuations, Doppler effects or photon density fluctuations, not taking into account the secondary effects nor the foregrounds.

from a *coupling* between the primary temperature fluctuation field and the mass concentration on the line of sight acting as deflectors. Their impact on the power spectrum has been investigated primarily by Blanchard & Schneider, (1987) who found the effect to be negligible. More recent works (Kashlinsky 1988, Cole & Efstathiou 1989, Sasaki 1989, Tomita & Watanabe 1989, Linder 1990, Cayón, Martínez-González & Sanz 1993a, b, Fukushige, Makino & Ebisuzaki 1994, Seljak 1996) eventually confirmed this conclusion, although the point was debated for a while. In particular Seljak (1996) made a detailed calculations of these effects for realistic models of CMB anisotropies and using a semi-analytic calculation based on a power spectrum approach that includes nonlinear corrections. In this text I will follow a rather similar approach to investigate the apparition of non-Gaussian features caused by weak lensing effects.

In section 2, I present the basis of the physical mechanisms describing the CMB map deformations induced by weak lensing effects. In Section 3, I give the explicit expression of the first non-vanishing correlation function, the four-point, in different remarkable geometries. In Section 4, quantitative predictions are given for two different cosmological models. The dependence of the results on the cosmological parameters, and the practical interests that such a measurement could have, are discussed in the last section.

2. Weak Lensing Effects on CMB Maps

2.1. The Basis of the Physical Mechanism

The effect of a gravitational lens is to induce a displacement of the light path, thus moving the apparent position of a sky patch on the last scattering surface by a given angle. The temperature of this patch is not affected itself, i.e. lenses do not created new structures, and a perfectly isotropic sky would remain so. The patch of the sky observed at the position $\gamma^{\text{obs.}}$ is thus actually coming from the position $\gamma^{\text{prim.}}$ on the "primordial sky", and the displacement, $\delta\gamma$, is induced by the mass concentration on the line of sight. More precisely $\delta\gamma$ is given by the transverse derivative of the projected potential ϕ of the mass fluctuations,

$$
\begin{aligned}
\delta\gamma &\equiv \qquad \gamma^{\text{prim.}}(\gamma) - \gamma^{\text{obs.}}(\gamma) \\
&= 2 \int_0^{\chi_{\text{CMB}}} \mathrm{d}\chi \, \frac{\mathcal{D}_0(\chi_{\text{CMB}}, \chi)}{\mathcal{D}_0(\chi_{\text{CMB}})} \nabla_\perp \phi(\chi),
\end{aligned} \tag{1}
$$

where $\mathcal{D}_0$ is the angular distance, χ is the distance of the lenses along the line of sight and χ_{CMB} is the distance of the last scattering surface (see Kaiser 1992, Seljak 1996, Bernardeau, van Waerbeke & Mellier 1996 for more details on this equation). It is interesting to rewrite this equation in terms of the Fourier transform of the *mass density fluc-*

tuation field. The Fourier transforms $\delta(\mathbf{k})$ are defined by,

$$
\begin{aligned}
\delta(\gamma, \chi) = \int \frac{\mathrm{d}^3\mathbf{k}}{(2\pi)^{3/2}} \, D_+(\chi) \, \delta(\mathbf{k}) \times \\
\exp\left[\mathrm{i}\mathcal{D}_0 \, \mathbf{k}_\perp \cdot \gamma + \mathrm{i}k_r \, \chi\right],
\end{aligned} \tag{2}
$$

where the linear growth factor $D_+(\chi)$ and the Fourier transforms are normalized to the present time. Then the potential reads,

$$
\begin{aligned}
\phi(\gamma, \chi) = \frac{3}{2}\Omega_0 \, \frac{D_+(\chi)}{a(\chi)} \int \frac{\mathrm{d}^3\mathbf{k}}{(2\pi)^{3/2}} \frac{\delta(\mathbf{k})}{k^2} \times \\
\exp\left[\mathrm{i}\mathcal{D}_0 \, \mathbf{k}_\perp \cdot \gamma + \mathrm{i}k_r \, \chi\right]
\end{aligned} \tag{3}
$$

which implies that the displacement can be written,

$$
\begin{aligned}
\delta\gamma \qquad &= \int_0^{\chi_{\text{CMB}}} \mathrm{d}\chi \, w(\chi) \int \frac{\mathrm{d}^3\mathbf{k}}{(2\pi)^{3/2}} \times \\
&\frac{\mathrm{i}\,\mathbf{k}_\perp}{k^2 \, \mathcal{D}_0(\chi)} \, \delta(\mathbf{k}) \, \exp\left[\mathrm{i}\mathcal{D}_0(\chi) \, \mathbf{k}_\perp \cdot \gamma + \mathrm{i}k_r \, \chi\right],
\end{aligned} \tag{4}
$$

with

$$
w(\chi) = 3\Omega_0 \, \frac{\mathcal{D}_0(\chi_{\text{CMB}} - \chi) \, \mathcal{D}_0(\chi)}{\mathcal{D}_0(\chi_{\text{CMB}})} \frac{D_+(\chi)}{a(\chi)}. \tag{5}
$$

The function $w(\chi)$ gives the efficiency function of lenses for sources located on the last scattering surface. It will be investigated in more details in the last section.

Note that in the following I will amply use the small angle approximation. It implies in particular that a given patch of the sky can be decomposed in flat waves and also that, in moment calculations, the component of $\mathbf{k}$ along the line of sight can be neglected compared to the norm of $\mathbf{k}_\perp$.

2.2. The Effects on CMB Maps

Compared to detections on background galaxies, the investigation of lens effects on the last scattering surface is very attractive, because this surface is at a well defined redshift, and has a negligible width. The analysis of the lens effects requires however more sophisticated tools since the induced shear cannot be directly measured. The primordial temperature patches on the CMB sky are indeed known only statistically and have a large angular correlation length. In which way, then, can the lens effects be revealed? Actually lensed CMB maps can be seen as collections of temperature patches of different sizes and shapes, which or only a fraction of which are displaced or deformed. Although this is slightly arbitrary, two effects can be distinguished in the way sizes and shapes of patches are affected,

- the *shear* effect that deforms, stretches out temperature patches in the shear direction,
- the *magnification* effect that globally enlarges or shrinks those patches.

The local deformations of the temperature patches are however a priori difficult to disentangle from the actual primordial intrinsic temperature fluctuations[2]. What will make then the effects detectable is the fact that *close* patches will be deformed in a *similar* way (when they are seen through a unique lens), and the excess of these close rare features cannot be accounted from a Gaussian field. It is thus possible to quantify their presence by statistical indicators. The power spectrum is of course not adapted to take into account the apparition of such non-Gaussian features. For that matter the high-order correlation functions, that are all identically zero for pure Gaussian fields, are extremely precious. Indeed these higher-order correlation functions contain informations about shapes, and their derivations can be pursued completely with Perturbation Theory techniques. In the following I focus my analysis on the first non vanishing correlation function, the four-point one.

3. The Effects of Weak Lensing on Temperature Correlation Functions

3.1. Statistical Properties

From the first equation it is easy to see that the temperature, $\delta_T^{\mathrm{obs.}}$, observed in the direction γ is in fact the unaffected temperature $\delta_T^{\mathrm{prim.}}$ coming from a slightly changed direction,

$$\delta_T^{\mathrm{obs.}}(\gamma^{\mathrm{obs.}}) = \delta_T^{\mathrm{prim.}}(\gamma^{\mathrm{prim.}}) = \delta_T^{\mathrm{prim.}}(\gamma^{\mathrm{obs.}} + \delta\gamma). \quad (6)$$

In the following I assume that the displacement is small compared to the angular scale at which the observations are made. This is a fair assumption since the displacement is at most of $1'$ (for cores of clusters) and that the angular resolution of the future satellite missions does not go below $10'$. As a result it is always possible to expand the relation (6) with respect to the displacement,

$$\delta_T^{\mathrm{obs.}}(\gamma) = \delta_T^{\mathrm{prim.}}(\gamma) + \frac{\partial}{\partial\gamma_i}\delta_T^{\mathrm{prim.}}(\gamma)\delta\gamma_i +$$
$$\frac{\partial^2}{\partial\gamma_i\partial\gamma_j}\delta_T^{\mathrm{prim.}}(\gamma)\delta\gamma_i\delta\gamma_j + \ldots \quad (7)$$

where the Einstein index summation prescription is used.

It is important to have in mind that both quantities $\delta_T^{\mathrm{prim.}}(\gamma)$ and $\delta\gamma$ are *independent* Gaussian fields. The primordial temperature field is Gaussian for inflationary scenario, and independent of the lens potential field because the last scattering surface is far from the intervening lenses (that will be found to be at redshift $\lesssim 5$). The lens potential field will be assumed to be in the linear regime, although this is not a crucial hypothesis[3].

---

[2]   In particular there are no known working method to construct weak-lensing maps from CMB temperature maps.
[3]   This assumption allows the use of the linear power spectrum, but one could have included nonlinear corrections to

In the following the correlation functions or moments will be calculated in the small angle approximation, for which the plane approximation for the last scattering surface can be made. Thus one can write,

$$\delta_T^{\mathrm{prim.}}(\gamma) = \int \frac{\mathrm{d}^2 l}{(2\pi)} a_l \exp(\mathrm{i} l \cdot \gamma), \quad (8)$$

where the a_l coefficients obey Gaussian statistical rules. In particular,

$$\langle a_l\, a_{l'} \rangle = \delta_{\mathrm{Dirac}}(l + l')\, C_l, \quad (9)$$

where the C_l are the "famous" C_l describing the angular power spectrum.

On the other hand the random variables $\delta(k)$ obey the statistics,

$$\langle \delta(k)\, \delta(k') \rangle = \delta_{\mathrm{Dirac}}(k + k')\, P(k), \quad (10)$$

where $P(k)$ is normalized to the present day. In order to produce a consistent set of power spectra it is important to have a consistent normalization for C_l and $P(k)$. This can be obtained from the small l behavior of C_l corresponding to the small k behavior of $P(k)$. In the following I will assume an Harrison-Zel'dovich initial spectrum, so that,

$$P(k) = A\, k \quad \text{at small } k. \quad (11)$$

The coefficient A can be related to the small l behavior of l (see Hu 1995 for instance),

$$l(l+1)\, C_l = \frac{A}{4\pi}\, \Omega_0^2 \left(\frac{a(\chi_{\mathrm{CMB}})}{D_+(\chi_{\mathrm{CMB}})}\right)^2 \quad \text{at small } l. \quad (12)$$

3.2. The Two-Point Correlation Function

The dominant corrective term for the angular two-point correlation function can be calculated from the expansion (7),

$$\langle \delta_T^{\mathrm{obs.}}(\gamma_1)\delta_T^{\mathrm{obs.}}(\gamma2) \rangle = \langle \delta_T^{\mathrm{prim.}}(\gamma_1)\delta_T^{\mathrm{prim.}}(\gamma2) \rangle + \quad (13)$$
$$\langle \frac{\partial}{\partial\gamma_i}\delta_T^{\mathrm{prim.}}(\gamma_1)\delta\gamma_i(\gamma_1)\, \frac{\partial}{\partial\gamma_j}\delta_T^{\mathrm{prim.}}(\gamma_2)\delta\gamma_j(\gamma_2) \rangle +$$
$$\langle \delta_T^{\mathrm{prim.}}(\gamma_1)\frac{\partial^2}{\partial\gamma_i\partial\gamma_j}\delta_T^{\mathrm{prim.}}(\gamma_2)\delta\gamma_i(\gamma_2)\delta\gamma_j(\gamma_2) \rangle + \ldots$$

The corrective terms have been written up to the quadratic term in the large-scale structure density field. The previous expression can be written in Fourier space,

$$\langle \delta_T^{\mathrm{obs.}}(\gamma_1)\delta_T^{\mathrm{obs.}}(\gamma2) \rangle = \int \frac{\mathrm{d}^2 l}{(2\pi)^2}\, C_l\, \exp[\mathrm{i} l \cdot \gamma_{12}] + \quad (14)$$
$$\int \frac{\mathrm{d}^2 l}{(2\pi)^2}\, C_l\, \exp[\mathrm{i} l \cdot \gamma_{12}] \int \mathrm{d}\chi_1 \mathrm{d}\chi_2\, w(\chi_1)\, w(\chi_2) \times$$
$$\int \frac{\mathrm{d}^3 k}{(2\pi)^3}\, P(k) \left(\frac{l \cdot k}{k^2\, \mathcal{D}_0(\chi_1)\, \mathcal{D}_0(\chi_2)}\right)^2 \exp[\mathrm{i}(\chi_1 - \chi_2)k_r] \times$$
$$\left(\exp[\mathrm{i}\mathcal{D}_0(\chi_1)k_\perp\cdot\gamma_1 - \mathrm{i}\mathcal{D}_0(\chi_2)k_\perp\cdot\gamma_2] - 2 \right)$$

it, since the lens density field is by no means required to be Gaussian.

where $\boldsymbol{\gamma}_{12}$ is the angular distance between $\boldsymbol{\gamma}_1$ and $\boldsymbol{\gamma}_2$, $\boldsymbol{\gamma}_{12} = |\boldsymbol{\gamma}_1 - \boldsymbol{\gamma}_2|$. This formula has been obtained using eqs. (9,10) defining the two power spectra. To complete the calculations one can use the small-angle approximation, well verified below 1 degree scale, which implies that

$$k \approx k_\perp \quad \text{and} \quad P(k) \approx P(k_\perp). \tag{15}$$

Then the integral over k_r leads to a Dirac function in $\chi_1 - \chi_2$. We eventually have,

$$\left\langle \delta_T^{\text{obs.}}(\boldsymbol{\gamma}_1) \delta_T^{\text{obs.}}(\boldsymbol{\gamma}2) \right\rangle = C(\boldsymbol{\gamma}_{12}) + \tag{16}$$
$$\int \frac{l\,\mathrm{d}l}{2\pi} \int \mathrm{d}\chi\, w^2(\chi) \int \frac{k\,\mathrm{d}k}{2\pi}\, P(k) \frac{l^2}{k^2\,\mathcal{D}_0^2(\chi)} \times$$
$$[(J_0(k\mathcal{D}_0\,\boldsymbol{\gamma}_{12}) - 1)\, J_0(l\,\boldsymbol{\gamma}_{12}) + J_2(k\mathcal{D}_0\,\boldsymbol{\gamma}_{12})\, J_2(l\,\boldsymbol{\gamma}_{12})],$$

with

$$C(\boldsymbol{\gamma}) = \int \frac{l\,\mathrm{d}l}{2\pi}\, C_l\, J_0(l\,\boldsymbol{\gamma}_{12}). \tag{17}$$

This result does not coincide apparently with the one of Seljak (1996, equation A.6), but simply because the exponential was not expanded in his expression. That this expansion can be done is amply justified by the fact that the displacements are small compared to the angular resolution scale. Then one recovers exactly the same expression. Note that the autocorrelation function of the displacement field is automatically introduced by the third term in (13).

3.3. Higher-Order Correlation Function

It is quite easy to see that the weak-lensing effects do not introduce a three-point correlation function. It is indeed impossible to build a term of non-zero ensemble average involving three a_l factors.

The first non trivial high order correlation function is thus the four-point correlation function. At this stage it is important to have in mind that the observable quantity is the *connected* part, $\left\langle \delta_T^{\text{obs.}}(\boldsymbol{\gamma}_1) \delta_T^{\text{obs.}}(\boldsymbol{\gamma}_2) \delta_T^{\text{obs.}}(\boldsymbol{\gamma}_3) \delta_T^{\text{obs.}}(\boldsymbol{\gamma}_4) \right\rangle_c$, of the ensemble average, $\left\langle \delta_T^{\text{obs.}}(\boldsymbol{\gamma}_1) \delta_T^{\text{obs.}}(\boldsymbol{\gamma}_2) \delta_T^{\text{obs.}}(\boldsymbol{\gamma}_3) \delta_T^{\text{obs.}}(\boldsymbol{\gamma}_4) \right\rangle$, that is the part which is obtained when the products of two point correlation functions that can be built have been subtracted out,

$$\left\langle \delta_T^{\text{obs.}}(\boldsymbol{\gamma}_1) \delta_T^{\text{obs.}}(\boldsymbol{\gamma}_2) \delta_T^{\text{obs.}}(\boldsymbol{\gamma}_3) \delta_T^{\text{obs.}}(\boldsymbol{\gamma}_4) \right\rangle_c \equiv \tag{18}$$
$$\left\langle \delta_T^{\text{obs.}}(\boldsymbol{\gamma}_1) \delta_T^{\text{obs.}}(\boldsymbol{\gamma}_2) \delta_T^{\text{obs.}}(\boldsymbol{\gamma}_3) \delta_T^{\text{obs.}}(\boldsymbol{\gamma}_4) \right\rangle -$$
$$\left\langle \delta_T^{\text{obs.}}(\boldsymbol{\gamma}_1) \delta_T^{\text{obs.}}(\boldsymbol{\gamma}_2) \right\rangle \left\langle \delta_T^{\text{obs.}}(\boldsymbol{\gamma}_3) \delta_T^{\text{obs.}}(\boldsymbol{\gamma}_4) \right\rangle -$$
$$\text{perm. (2 other terms)}.$$

The connected part is obviously zero for the primordial field: it is a direct consequence of its Gaussian nature. The dominant term, in terms of weak lensing effects, is thus given by,

$$\left\langle \delta_T^{\text{obs.}}(\boldsymbol{\gamma}_1) \delta_T^{\text{obs.}}(\boldsymbol{\gamma}_2) \delta_T^{\text{obs.}}(\boldsymbol{\gamma}_3) \delta_T^{\text{obs.}}(\boldsymbol{\gamma}_4) \right\rangle_c \equiv \tag{19}$$

$$\left\langle \delta_T^{\text{obs.}}(\boldsymbol{\gamma}_1)\, \frac{\partial}{\partial\boldsymbol{\gamma}_i}\delta_T^{\text{prim.}}(\boldsymbol{\gamma}_2) \right\rangle \left\langle \boldsymbol{\delta\gamma}_i(\boldsymbol{\gamma}_2)\, \boldsymbol{\delta\gamma}_j(\boldsymbol{\gamma}_3) \right\rangle \times$$
$$\left\langle \frac{\partial}{\partial\boldsymbol{\gamma}_j}\delta_T^{\text{prim.}}(\boldsymbol{\gamma}_3)\, \delta_T^{\text{obs.}}(\boldsymbol{\gamma}_4) \right\rangle + \text{perm. (11 other terms)}.$$

Roughly speaking it means that the four-point correlation function, in units of the square of the second, is proportional to the weak lensing angular correlation function. Although at this stage it is difficult to give definitive quantitative predictions, the magnitude of the fourth order correlation function should be about 10^{-2} (the order of the corrective term in [13]), which should be easily detectable in full sky coverage CMB maps. The expression of the four-point correlation function can be given in terms of the power spectra,

$$\left\langle \delta_T^{\text{obs.}}(\boldsymbol{\gamma}_1) \delta_T^{\text{obs.}}(\boldsymbol{\gamma}_2) \delta_T^{\text{obs.}}(\boldsymbol{\gamma}_3) \delta_T^{\text{obs.}}(\boldsymbol{\gamma}_4) \right\rangle_c = \tag{20}$$
$$\int \frac{\mathrm{d}^2\boldsymbol{l}_1}{(2\pi)^2\, C_{l_1}} \int \frac{\mathrm{d}^2\boldsymbol{l}_2}{(2\pi)^2\, C_{l_2}} \int \mathrm{d}\chi\, w^2(\chi) \int \frac{\mathrm{d}^2\boldsymbol{k}}{(2\pi)^2}\, P(k)$$
$$\frac{\boldsymbol{l}_1 \cdot \boldsymbol{k}}{k^2\,\mathcal{D}_0} \frac{\boldsymbol{l}_1 \cdot \boldsymbol{k}}{k^2\,\mathcal{D}_0}\, \exp\left[\mathrm{i}\boldsymbol{l}_1 \cdot \boldsymbol{\gamma}_{12} + \mathrm{i}\mathcal{D}_0\boldsymbol{k} \cdot \boldsymbol{\gamma}_{23} + \mathrm{i}\boldsymbol{l}_2 \cdot \boldsymbol{\gamma}_{34}\right] +$$
$$\text{perm. (11 other terms)}.$$

This expression can be calculated with an integration over the angles between $\boldsymbol{l}_1$ and $\boldsymbol{\gamma}_{12}$ and $\boldsymbol{l}_2$ and $\boldsymbol{\gamma}_{34}$ respectively. It yields the Bessel functions $J_1(l_1\,\boldsymbol{\gamma}_{12})$ and $J_1(l_2\,\boldsymbol{\gamma}_{34})$. The results can thus be expressed in terms of the angular derivative of the two-point correlation function,

$$\frac{\mathrm{d}}{\mathrm{d}\boldsymbol{\gamma}}C(\boldsymbol{\gamma}) = -\int \frac{l^2\mathrm{d}l}{2\pi}\, C_l\, J_1(l\boldsymbol{\gamma}), \tag{21}$$

and with quantities associated with the angular correlation of the displacement field,

$$D_p(\boldsymbol{\gamma}) = \int \mathrm{d}\chi\, w^2(\chi) \int \frac{k\,\mathrm{d}k}{2\pi}\, \frac{P(k)}{k^2\,\mathcal{D}_0^2}\, J_p(\mathcal{D}_0\, k\,\boldsymbol{\gamma}), \tag{22}$$

leading to (Appendix A),

$$\left\langle \delta_T^{\text{obs.}}(\boldsymbol{\gamma}_1) \delta_T^{\text{obs.}}(\boldsymbol{\gamma}_2) \delta_T^{\text{obs.}}(\boldsymbol{\gamma}_3) \delta_T^{\text{obs.}}(\boldsymbol{\gamma}_4) \right\rangle_c = \tag{23}$$
$$\frac{1}{2} \frac{\mathrm{d}}{\mathrm{d}\boldsymbol{\gamma}}C(\boldsymbol{\gamma}_{12}) \frac{\mathrm{d}}{\mathrm{d}\boldsymbol{\gamma}}C(\boldsymbol{\gamma}_{34}) \times$$
$$[D_0(\boldsymbol{\gamma}_{23}) \cos(\varphi_{12} - \varphi_{34}) - D_2(\boldsymbol{\gamma}_{23}) \cos(\varphi_{12} + \varphi_{34})] +$$
$$+ \text{perm. (11 other terms)},$$

where φ_{12} is the angle between $\boldsymbol{\gamma}_{12}$ and $\boldsymbol{\gamma}_{23}$ and φ_{34} is the angle between $\boldsymbol{\gamma}_{43}$ and $\boldsymbol{\gamma}_{32}$ (see Fig. 1). Two terms are thus involved. The a priori dominant term is the one in D_0, and it is weighted by the cosine of the angle $\varphi_{12} - \varphi_{34} \equiv \psi$ (see Fig. 1), that is the angle between the directions $\boldsymbol{\gamma}_{12}$ and $\boldsymbol{\gamma}_{34}$ on the sky. It gives a clear geometrical dependence for the four point-correlation function. However, one should have in mind that 11 other terms have to be taken into account in this calculation. This signal may therefore be masked by other geometric dependences.
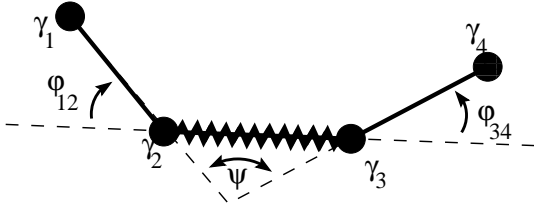
Fig. 1. Description of the angles intervening in the expression (24) of the four-point correlation function. The thick solid line materializes the $\mathrm{d}\,C(\theta)/\mathrm{d}\,\theta$ factor, whereas the hatched lines represents the correlation functions of the displacement field.

Quantitative calculations can be done for specific cosmological models (see next section). However, one obvious problem for a practical determination of this correlation function is that it depends on 5 different variables. It is thus crucial to reduce the number of variables by considering simplified geometries.

3.4. Peculiar Geometries

3.4.1. When two Directions Coincide

The first geometry one may think of is when two points are merged together, that is the expression of $\left\langle \delta_T^{\mathrm{obs.}}(\boldsymbol{\gamma}_1) \left[\delta_T^{\mathrm{obs.}}(\boldsymbol{\gamma}_2)\right]^2 \delta_T^{\mathrm{obs.}}(\boldsymbol{\gamma}_3)\right\rangle_c$. This notation is actually a bit oversimplified since the local temperature fluctuations are actually filtered by the used apparatus. One should thus have in mind that the two directions denoted $\boldsymbol{\gamma}_2$ are actually close random directions in a beam centered on $\boldsymbol{\gamma}_2$.

Of course, once again, many terms are contributing to this ensemble average but I will first concentrate on the case where the connection between the two $\delta_T^{\mathrm{obs.}}(\boldsymbol{\gamma}_2)$ is made by the lens coupling term (subsection A.2.b). In such a case one can see that ψ is given by the angle between $\boldsymbol{\gamma}_2 - \boldsymbol{\gamma}_1$ and $\boldsymbol{\gamma}_3 - \boldsymbol{\gamma}_2$ and is not affected by the smoothing. This is not the case for the term in $\cos(\varphi_{12} + \varphi_{34})$ which is expected to vanish because it is averaged to zero (more precise derivations are given in the Appendix). This contribution is thus proportional to the cosine of the angle, and to the autocorrelation function of the displacement field.

What about the other terms? Their geometrical representations are given in Fig. 2. The (2a) diagram is the term that has just been considered and is expected to dominate the final expression. Note that all these diagrams have a symmetry factor of 2 compared to what is given in the Appendix. At first view the (2b) diagram vanishes because φ_{12} takes a random value averaging both $\cos(\varphi_{12} - \varphi_{34})$ and $\cos(\varphi_{12} + \varphi_{34})$ to zero. A more detailed calculation is proposed in the Appendix. It shows that it gives a contribution proportional to the angular correlation function of
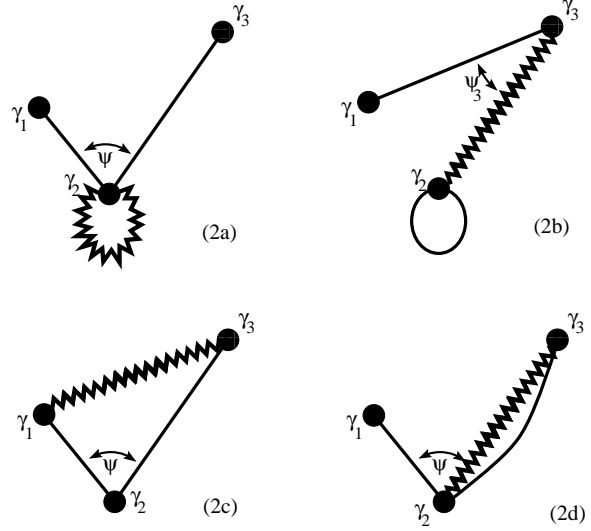

Fig. 2. Geometrical representation of the terms intervening in the expression (25).

the local weak lensing convergence (see Blandford et al. 1991, Villumsen 1996, Bernardeau et al. 1996),

$$M_0(\boldsymbol{\gamma}) = \int \mathrm{d}\chi\, w^2(\chi) \int \frac{k\,\mathrm{d}k}{2\pi}\, P(k)\, J_0(\mathcal{D}_0\, k\, \boldsymbol{\gamma}). \qquad (24)$$

The two other diagrams are simpler since they can be simply obtained from the general expression (24). Taking all these terms into account we have,

$$\left\langle \delta_T^{\mathrm{obs.}}(\boldsymbol{\gamma}_1) \left[\delta_T^{\mathrm{obs.}}(\boldsymbol{\gamma}_2)\right]^2 \delta_T^{\mathrm{obs.}}(\boldsymbol{\gamma}_3)\right\rangle_c \approx \qquad (25)$$

$$\frac{\mathrm{d}\log(\overline{C})}{\mathrm{d}\log(\theta_0)}\, \frac{\mathrm{d}}{\mathrm{d}\boldsymbol{\gamma}}\, C(\boldsymbol{\gamma}_{13})\, \left[\boldsymbol{\gamma}_{12}\, M_0(\boldsymbol{\gamma}_{12})\, \cos(\psi_1) + \right.$$

$$\boldsymbol{\gamma}_{23}\, M_0(\boldsymbol{\gamma}_{23})\, \cos(\psi_3)\big] +$$

$$\frac{\mathrm{d}}{\mathrm{d}\boldsymbol{\gamma}}C(\boldsymbol{\gamma}_{12})\, \frac{\mathrm{d}}{\mathrm{d}\boldsymbol{\gamma}}C(\boldsymbol{\gamma}_{23})\, \cos(\psi) \times$$

$$\left[\overline{D}_0(\theta_0) + D_0(\boldsymbol{\gamma}_{13}) - D_0(\boldsymbol{\gamma}_{12}) - D_0(\boldsymbol{\gamma}_{23})\right]$$

where ψ_3 is shown on Fig. (2b) (ψ_1 corresponds to the diagram obtained when the roles of $\boldsymbol{\gamma}_1$ and $\boldsymbol{\gamma}_3$ are inverted) and θ_0 is the smoothing angle of the experiment. In this expression, the D_2 terms have been neglected, D_0 has been changed in $\overline{D}_0$ for diagram (2a) and C in $\overline{C}$ in (2b). This is due to the filtering effects. One should indeed take into account the average displacement within the beam size of the experiment in the first case, the rms temperature fluctuations in the second. More precisely we have,

$$\overline{D}_0(\theta) = \int \mathrm{d}\chi\, w^2(\chi) \int \frac{k\,\mathrm{d}k}{2\pi}\, \frac{P(k)}{k^2\, \mathcal{D}_0^2}\, W^2(\mathcal{D}_0\, k\, \theta), \qquad (26)$$

and

$$\overline{C}(\theta) = \int \frac{l\,\mathrm{d}l}{2\pi}\, C_l\, W^2(l\, \theta), \qquad (27)$$

with, for a top-hat window function for instance,

$$W(x) = \frac{2J_1(x)}{x}. \tag{28}$$

It is then interesting to define the function,

$$\kappa_4(\boldsymbol{\gamma}_{12}, \boldsymbol{\gamma}_{23}) = \tag{29}$$
$$\frac{\left\langle \delta_T^{\text{obs.}}(\boldsymbol{\gamma}_1) \left[\delta_T^{\text{obs.}}(\boldsymbol{\gamma}_2)\right]^2 \delta_T^{\text{obs.}}(\boldsymbol{\gamma}_3)\right\rangle_c}{\left\langle \delta_T^{\text{obs.}}(\boldsymbol{\gamma}_1) \delta_T^{\text{obs.}}(\boldsymbol{\gamma}_2)\right\rangle \left\langle \delta_T^{\text{obs.}}(\boldsymbol{\gamma}_2) \delta_T^{\text{obs.}}(\boldsymbol{\gamma}_3)\right\rangle},$$

which is a dimensionless quantity. It does not depend in particular on the magnitude of the CMB temperature fluctuations and it is directly proportional to the large-scale structure power spectrum, with a known dependence on the shape of the anisotropy power spectrum. This quantity would thus be a measure the weak lensing effects in CMB maps. Taking into account the fact that the diagram (2b) generally leads to a negligible contribution we have,

$$\kappa_4(\boldsymbol{\gamma}_{12}, \boldsymbol{\gamma}_{23}) \approx \tag{30}$$
$$\frac{\mathrm{d}}{\mathrm{d}\boldsymbol{\gamma}} \log[C(\boldsymbol{\gamma}_{12})] \frac{\mathrm{d}}{\mathrm{d}\boldsymbol{\gamma}} \log[C(\boldsymbol{\gamma}_{23})] \cos(\psi) \times$$
$$\left[\overline{D}_0(\theta_0) + D_0(\boldsymbol{\gamma}_{13}) - D_0(\boldsymbol{\gamma}_{12}) - D_0(\boldsymbol{\gamma}_{23})\right].$$

A 2D contour plot of the function $\kappa_4(\boldsymbol{\gamma}_{12}, \boldsymbol{\gamma}_{23})$ is proposed in Fig. 6 for a peculiar cosmological case.

The main contribution to this expression is the term coming from the diagram (2a), but the contributions from (2c) and (2d) cannot be neglected because the correlation function of the displacement field D_0 is only slowly decreasing with the angle (see next section). It is interesting to have in mind the physical effect described by this result. It corresponds indeed to a shear effect that is the *deformation of two nearby temperature patches by a single lens*. It can thus be seen as the excess of close temperature peaks that are elongated in the *same* direction. It is therefore logical that this effect is proportional to the correlation function of the displacement field. However, it does not always dominated the four point correlation function. This is the case in particular at the degree scale since the derivative of the temperature correlation function vanishes (see Fig. 4 in the next Section). The next subsection is devoted to a simpler geometry where this case is more specifically investigated.

3.4.2. When two Pairs Coincide

This case is obtained from the previous case when the directions $\boldsymbol{\gamma}_3$ and $\boldsymbol{\gamma}_4$ coincide. The geometrical representations of the involved terms are presented in Fig. 3. The a priori dominant term corresponds to the diagram (3b). However, as noted previously, both the diagrams (3b) and (3c) vanish for specific values of the distance between $\boldsymbol{\gamma}_1$ and $\boldsymbol{\gamma}_2$. In such a case we are left with the diagram (3a). A crude evaluation of this diagram gives zero because the

Fig. 3. Geometrical representation of the terms intervening in the expression (31).

averages over the angles φ_{12} and φ_{34} are expected to vanish. However this is true only when the smoothing angle is negligible compared to the angular distance between $\boldsymbol{\gamma}_1$ and $\boldsymbol{\gamma}_2$. More precise calculations (subsection A.3) show that this term is proportional to the logarithmic derivative of the temperature variance in the beam. The resulting value of the correlation function is (taking into account a symmetry factor of 4),

$$\left\langle \left[\delta_T^{\text{obs.}}(\boldsymbol{\gamma}_1)\right]^2 \left[\delta_T^{\text{obs.}}(\boldsymbol{\gamma}_2)\right]^2 \right\rangle_c \approx \tag{31}$$
$$\frac{1}{4}\left(\theta_0 \frac{\mathrm{d}\overline{C}(\theta_0)}{\mathrm{d}\theta}\right)^2 M_0(\boldsymbol{\gamma}_{12}) + \left[\frac{\mathrm{d}}{\mathrm{d}\boldsymbol{\gamma}} C(\boldsymbol{\gamma}_{12})\right]^2 \times$$
$$\left[\overline{D}_0(\theta_0) - D_0(\boldsymbol{\gamma}_{12})\right].$$

Note that the first term is no more proportional to the angular correlation of the displacement field, but to the angular correlation of the convergence (that is, within a factor 2, of the magnification in the weak lensing regime). Here the physical mechanism has changed. The correlation function is not due to a local shear, but to single lens amplification of patches on the primordial sky that create an *excess of close bright peaks*. It is thus clearly a magnification effect.

3.4.3. When the four Directions Coincide

The last case I consider is when the four directions coincide. In this case the magnification effect always dominates and the results, obtained in subsection A.4, are similar to the one discussed in the previous subsection, but with small changes introduced by the filtering effects,

$$\left\langle \left[\delta_T^{\text{obs.}}(\theta_0)\right]^4 \right\rangle_c = \frac{3}{4}\left(\theta_0 \frac{\mathrm{d}\overline{C}(\theta_0)}{\mathrm{d}\theta}\right)^2 \overline{M}_0(\theta_0) \tag{32}$$

with

$$\overline{M}_0(\theta_0) = \int \mathrm{d}\chi \, w^2(\chi) \int \frac{k \, \mathrm{d}k}{2\pi} P(k) W^2(\mathcal{D}_0 \, k \, \theta_0). \tag{33}$$

This result has been properly demonstrated for a top-hat window function, and should be roughly correct for other window functions. Note that this expression is also the fourth cumulant of the local filtered temperature probability distribution function. We can as well define the dimensionless quantity,

$$\kappa_4(\theta_0) = \frac{\left\langle \left[\delta_T^{\mathrm{obs.}}(\theta_0)\right]^4 \right\rangle_c}{\left\langle \left[\delta_T^{\mathrm{obs.}}(\theta_0)\right]^2 \right\rangle^2} \approx \frac{3}{4} \left(\frac{\mathrm{d}\log[\overline{C}(\theta_0)]}{\mathrm{d}\log[\theta]} \right)^2 \overline{M}_0(\theta_0) \quad (34)$$

which tells us that *the dimensionless kurtosis of the local filtered CMB temperature probability distribution function is proportional to the variance of the local filtered convergence.*

4. Quantitative Predictions

4.1. The Cosmological Models

The cosmological models used to illustrate the previous results by quantitative predictions are standard CDM models with $\Omega_{\mathrm{baryon}} = 0.05$, $H_0 = 50 \ km/s/$Mpc with an initial Harrison-Zel'dovich spectrum. Two cases have been chosen, $\Omega_0 = 1$, $\Lambda = 0$ (model 1) and $\Omega_0 = 0.3$, $\Lambda = 0.7$ (model 2). The transfer function and temperature power spectrum were both computed with the code of Seljak & Zaldarriaga (1996).

For convenience the mass fluctuation power spectra were approximated by simple analytic fits (similar to the ones proposed by Bond & Efstathiou 1984),

$$P(k) = A \frac{k}{\left(1 + \left[a\,k + (b\,k)^{3/2} + (c\,k)^2\right]^u\right)^{2/u}}, \quad (35)$$

with

$$u = 1.13;$$
$$a = \frac{6.5}{3000\ \Gamma};$$
$$b = \frac{3}{3000\ \Gamma};$$
$$c = \frac{1.7}{3000\ \Gamma};$$

and

$$\Gamma = 0.5 \ \ \text{for} \ \Omega_0 = 1.0$$
$$\Gamma = 0.13 \ \ \text{for} \ \Omega_0 = 0.3.$$

The normalization factor is given by the relation (12) with observational constraints,

$$l(l+1)\,C_l = \frac{24\pi}{5} \left(\frac{Q_0}{T_0} \right)^2. \quad (36)$$

The measured values of Q_0 and T_0 by the COBE satellite (Mather et al. 1994, Gorski et al. 1994)

$$T_0 = 2.726 \pm 0.010 \ K, \quad (37)$$
$$Q_0 = 19.9 \pm 1.6\ 10^{-6} \ K, \quad (38)$$

provide the normalization constraint for A,

$$A \approx 1.01\ 10^{-8}\ \Omega_0^{-2} \left(\frac{a(\chi_{\mathrm{CMB}})}{D_+(\chi_{\mathrm{CMB}})} \right)^2. \quad (39)$$

Note that in the previous equations, distance units have been chosen so that $c\,H_0 = 1$.
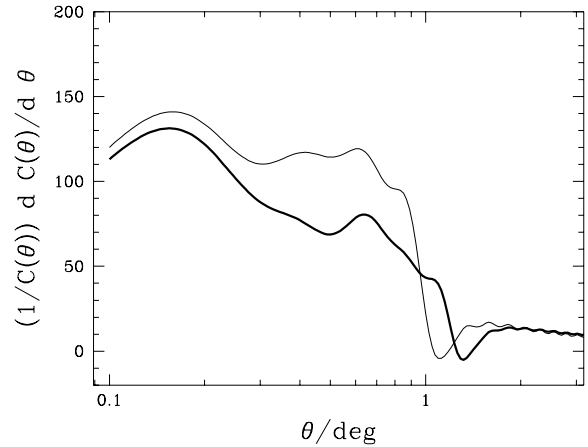
4.2. Numerical Results

Fig. 4. The function $1/C(\theta)\ \mathrm{d}C(\theta)/\mathrm{d}\theta$ as a function of the angle. The thick line is for model 1 and the thin line for model 2

I present the derivatives of the temperature angular correlation functions in Fig. 4. They exhibit a remarkable property, since they both drop to zero at a scale slightly larger than 1 degree. This property can be of great help to disentangle various contributions. For instance it implies that specific geometries produce a vanishing four-point correlation function. This is the case for instance when three of the four directions form an equilateral triangle with ~ 1.2 deg of side length. Such a property could be of crucial interest to ascertain the origin of an observed four-point correlation function.

The two other quantities of interest are the functions $D_0(\boldsymbol{\gamma})$, $D_2(\boldsymbol{\gamma})$ and $\overline{D}_0(\boldsymbol{\gamma})$ (eqs. 22, 26) that describe the magnitude of the lens effects. They are presented in Fig. 5. One can see that D_0 and $\overline{D}_0$ dominate at small scale. The resulting shape of the dimensionless four-point correlation function $\kappa_4(\boldsymbol{\gamma}_{12}, \boldsymbol{\gamma}_{23})$ (eq. 29) is presented in Fig. 6. It exhibits specific features induced by the $\cos(\psi)$ factor and by the derivative of the temperature angular correlation function. The fact that the latter vanishes is clearly present with a significant circular feature at 1 degree scale. It implies that the kurtosis is maximum for angular distances below 1 degree. Note that in this figure, all contributions have been included, but the contributions from (2b) are found to be negligible and not to affect the global features of this plot.
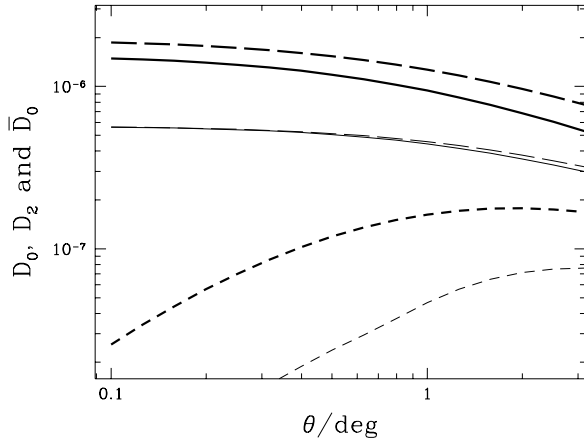
Fig. 5. The functions D_0 (solid lines), D_2 (dashed lines) and $\overline{D}_0$ (long dashed lines) for model 1 (thick lines) and model 2 (thin lines).
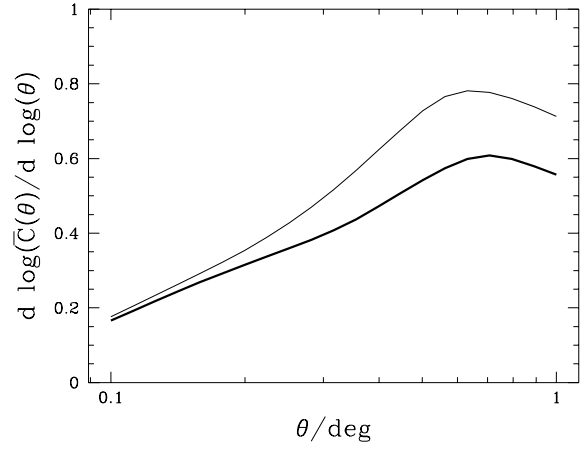

Fig. 7. The functions $\mathrm{d}\log[\overline{C}(\theta)]/\mathrm{d}\log[\theta]$ for model 1 (thick line) and model 2 (thin line)
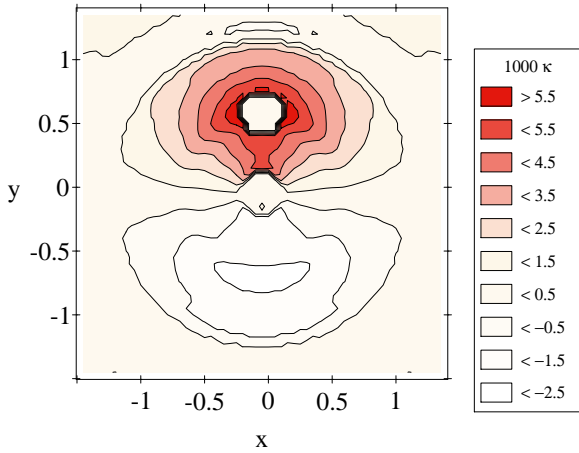

Fig. 6. Contour plot of the function $\kappa_4(\gamma_{12}, \gamma_{23})$ (eq. 29) as a function of the relative position (in degrees) of γ_3 when γ_2 is the central point of the graph and γ_1 is at the coordinates $x = 0$, $y = +0.63\,\mathrm{deg}$. The value of κ_4 has been multiplied by 1000.

Fig. 8. The functions M_0 (solid lines) and $\overline{M}_0$ (dashed lines) for model 1 (thick lines) and model 2 (thin lines)

I also present the quantities intervening in the expression of the dimensionless kurtosis of the CMB temperature PDF. The index of the local temperature fluctuations is given in Fig. 7 for the two cosmological models. The variance of the convergence is presented in Fig. 8, and the resulting value of κ_4 in Fig. 9.

The resulting coefficient κ_4 can be as high as $5\ 10^{-3}$. It depends however a lot on the cosmological models and more particularly on the amount of power at about $10\,h^{-1}\mathrm{Mpc}$ scale. The reason why $\overline{M}_0$, and consequently κ_4, is smaller for the $\Omega = 0.3$ case is thus actually due to the change of shape of $P(k)$ (i.e., a lower value of Γ), and not directly to the low value of Ω. The dependence on the cosmological parameters is investigated in more details in the next subsection.
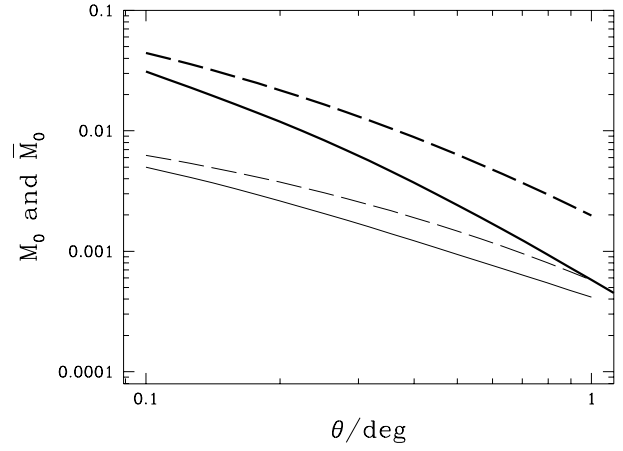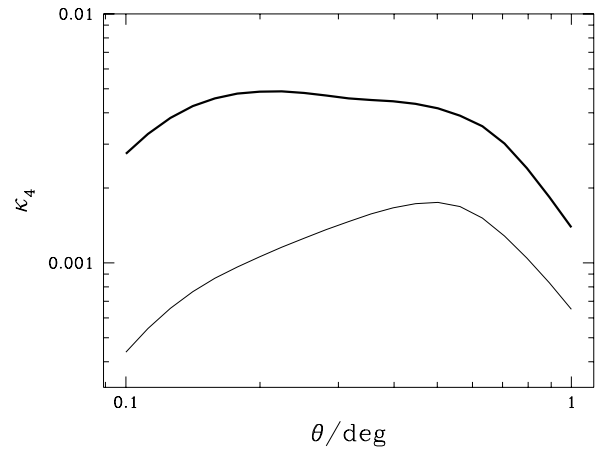

Fig. 9. The function $\kappa_4(\theta)$ (eq. 34) for model 1 (thick line) and model 2 (thin line)

4.3. Dependence on the Cosmological Parameters

The dependence on the cosmological parameters enters in various aspects. It is important in particular for the relation between the C_l and the mass fluctuation power spectrum $P(k)$. This is not the aim of this paper to explore in great details all these dependences. There is however a dependence which is specific of the lens effects, that is the shape of the efficiency function $w(z)$ (eq. 5). In Fig. 10, I present the function $w(z)$ for different cosmological models. We can see that both the shape and the amplitude of this function strongly depend on the cosmological parameters.

The main dependence is actually due to the factor Ω appearing in the expression of $w(z)$. This is however quite misleading since this factor cancels out with the one intervening in the expression of the normalization factor A (eq. 39). The dependence on the cosmological parameters is thus mainly contained in the shape of the power spectrum, that is in the ratio between the amount of power at relatively small scale to the power at very large scale, although they enter significantly in the efficiency function $w(z)$, even when the overall Ω factor has been dropped. The way the two cosmological parameters Ω_0 and Λ enter in this expression is unfortunately rather cumbersome. It is however clear that the CMB four-point correlation function contains informations on the cosmological parameters in a quite different combination compared to the one intervening in the temperature power spectrum. In particular the detection of such an affect may allow to better disentangle what is specific of C_l from what contribute directly to $P(k)$.
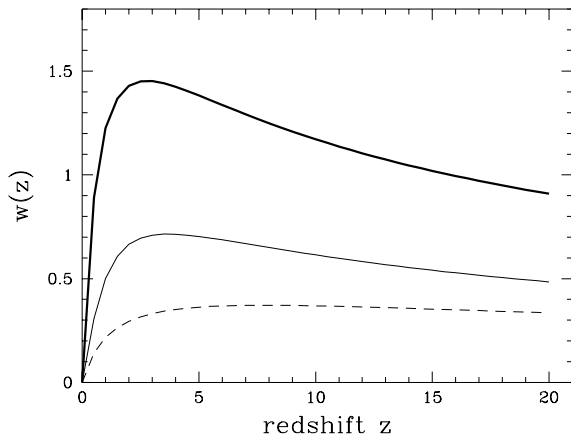

Fig. 10. The function $w(z)$ (eq. 5) for the Einstein-de Sitter case (thick solid line), a model with $\Omega = 0.3$, $\Lambda = 0.7$ (thin solid line) and a model with $\Omega = 0.3$, $\Lambda = 0$ (dashed line).

5. Discussion and Conclusions

In this work, I have calculated the expression of the four-point temperature correlation function as induced by weak-lensing effects. For standard CDM model, the amplitude of this correlation function, in units of the square of the second, is found to be of order of $5 \ 10^{-3}$. However, this estimation did not take into account the nonlinear evolution of the power spectrum that might significantly amplify this signal at small angular scale. This is for instance what is predicted for the two-point correlation function of the polarization of background galaxies (Jain & Seljak 1996). Unfortunately, in the case of CMB maps, the scale at which this effect might appear cannot be deduced straightforwardly from this work. This effect is indeed the result of a line of sight integration that mix different scales and different redshifts for a given selection function (e.g. Fig. 10) which is itself dependent on the redshift of the sources. Moreover all the intervening quantities have non trivial dependences on the cosmological parameters that should be taken into account. A detailed examination of the nonlinear effects is then left for a forthcoming paper.

I would like to stress, that the amplitude of the lensing effects should be large enough to be detectable, at least marginally, in full sky CMB anisotropy measurements. The possibility of doing such measurements is directly related to the cosmic noise associated with the quantities of interest, fourth moment or four-point correlation function. So far, no precise estimation of the cosmic noise for the four-point correlation function has been made, but following Srednicki (1993), who presented the calculation for the three-point correlation function, one expects the cosmic variance of those quantities to be of the order of $1/l_{\rm pk.}$ where $l_{\rm pk.}$ is the typical value of l contributing to the temperature fluctuations. One can observe that the value of $1/l_{\rm pk.}$ is of the order of the signal, however, one should have in mind that a direct and too naive calculation of the cosmic noise may be actually misleading since the long wavelength fluctuations (corresponding to the low l part of the power spectrum) contribute significantly to it, whereas the lensing signal originates mainly from the small angular scales (below 1 degree). It suggests that the weak lensing signal might be more easily detectable in maps where the long wavelength temperature fluctuations have been removed. Moreover the detailed methods used to extract the signal might also be of different robustness against the cosmic noise. In particular, it could be fruitful to take advantage of the a priori knowledge of the geometrical dependence of the four-point correlation function (see for example the $cos(\psi)$ factor in the expression [30]). In a forthcoming paper, we explore the different possible strategies for the data analysis, and will present detailed estimations of the precision at which such a detection could be made in the future satellite missions.

It also has to be noted that other secondary effects or foregrounds may also contribute to the four-point correlation function, not to mention the case of more exotic cosmological models based on intrinsically non-Gaussian topological defects. In particular the nonlinear Doppler effects could induce a significant four-point correlation func-

tion, because it is caused by intrinsically non-Gaussian objects. There are however no reasons for these effects to have the same geometrical dependences, $\cos(\psi)$ factor and dependence on the shape of the temperature two-point correlation function. Hence, it should be possible to distinguish this effect from other sources.

The most exciting aspect of this analysis is probably that the magnitude of the effect depends on the cosmological parameters, Ω, Λ and $P(k)$ in a known way. The detection of the temperature four-point correlation function may thus reveal to be extremely precious to test the global picture of the large-scale structure formation, as it will be unveiled by CMB anisotropy measurements.

Acknowledgments

References

Bernardeau, F. 1995, A&A, 301, 309.
Bernardeau, F., van Waerbeke, L. & Mellier, Y. 1996, submitted to A&A, astro-ph/9609122
Blanchard, A. & Schneider, J. 1987, A&A, 184, 1
Blandford, R. D., Saust, A. B., Brainerd, T. G., Villumsen, J. V. 1991, MNRAS 251, 600.
Bond, J.R., Efstathiou, G. 1984, MNRAS, 285, L45
Bond, J.R., Efstathiou, G. 1987, MNRAS, 226, 655
Bouchet, F., Juszkiewicz, R., Colombi, S. & Pellat, R. 1992, ApJ, 394, L5
Cayón, L., Martínez-González, E. & Sanz, J.L. 1993a, ApJ, 403, 471
Cayón, L., Martínez-González, E. & Sanz, J.L. 1993b, ApJ, 413, 10
Cobras/Samba phase A report, 1996, http://astro.estec.esa.nl/SA-general/Projects/Cobras/cobras.html
Cole, S. & Efstathiou, G. 1989, MNRAS, 239, 195
Falk, T., Rangarajan, R. & Srednicki, M. 1993, ApJ, 403, L1
Fukushige, T., Makino, J. & Ebisuzaki, T. 1994, ApJ, 436, L107
Gorski, K.M. et al. ApJ, 1994, 430, L89
Gradshteyn, I.S. & Ryzhik J.M. 1980, Table of Integrals, Series and Products (New-York; Academics)
Hu, W., 1995, PhD Thesis, UC Berkeley, astro-ph/9508126
Jain, B. & Seljak, U. 1996, astro-ph/9611077
Jungman, G., Kamionkowski, M., Kosowsky, A. & Spergel, D.N., 1996, astro-ph/9512139
Kaiser, N. 1992, ApJ, 388, 272
Kashlinsky, A. 1988, ApJ, 331, L1
Linder, V.E., 1990, MNRAS, 243, 353
Mather, J.C. et al. 1994, ApJ, 420, 439
Munshi, D., Souradeep, T. Starobinsky, A. 1995, ApJ, 454, 552
Sasaki, M. 1989, MNRAS, 240, 415
Srednicki, M. 1993, ApJ, 416, L1
Seljak, U. 1996, ApJ 463, 1.
Seljak, U. & Zaldarriaga, M. 1996, ApJ, 469, 437
Tomita, K. & Watanabe, K. 1989, Prog. Theor. Phys., 82, 563
Villumsen, J. V. 1996, MNRAS 281, 369.

Appendix A: Calculation of the Filtering Effects

In this appendix I explicitly take into account the filtering effects to compute the expressions of the four-point correlation function in different geometries. The filtering can be the one due to the angular resolution of the apparatus or due to a subsequent filtering of the temperature field. When it needs to be specified the adopted window function will always be the angular top-hat window function.

The expression I am interested in is the expression (19) where $\boldsymbol{\gamma}^{\mathrm{prim.}}$ and the coupling term $\nabla\boldsymbol{\gamma}^{\mathrm{prim.}} \cdot \boldsymbol{\delta\gamma}$ are given by,

$$\delta_T^{\mathrm{prim.}}(\boldsymbol{\gamma}) = \int \frac{\mathrm{d}^2\boldsymbol{l}}{(2\pi)^2} \, a_l \, W(l\,\theta_0) \, e^{\mathrm{i}\boldsymbol{l}\cdot\boldsymbol{\gamma}}, \tag{40}$$

and,

$$\nabla\boldsymbol{\gamma}^{\mathrm{prim.}}(\boldsymbol{\gamma}) \cdot \boldsymbol{\delta\gamma} = \tag{41}$$
$$\int \frac{\mathrm{d}^2\boldsymbol{l}}{(2\pi)^2} \, a_l \, W(l\theta_0) \int \mathrm{d}\chi \, w(\chi) \int \frac{\mathrm{d}^2\boldsymbol{k}}{(2\pi)^2} \times$$
$$a_l \, \delta(\boldsymbol{k}) \, \frac{\boldsymbol{l}\cdot\boldsymbol{k}}{k^2\,\mathcal{D}_0} \, W\left(|\boldsymbol{l} + \mathcal{D}_0\,\boldsymbol{k}|\,\theta_0\right) \; \exp[\mathrm{i}(\boldsymbol{l} + \mathcal{D}_0\boldsymbol{k})\cdot\boldsymbol{\gamma}],$$

where θ_0 is the smoothing angle. The quantity of interest is thus

$$C_4(\boldsymbol{\gamma}_1, \boldsymbol{\gamma}_2, \boldsymbol{\gamma}_3, \boldsymbol{\gamma}_4) = \int \frac{\mathrm{d}^2\boldsymbol{l}_1}{(2\pi)^2} \, C_{l_1} \int \frac{\mathrm{d}^2\boldsymbol{l}_2}{(2\pi)^2} \, C_{l_2} \times \tag{42}$$
$$\int \mathrm{d}\chi \, w^2(\chi) \int \frac{\mathrm{d}^2\boldsymbol{k}}{(2\pi)^2} \, P(k) \, W(l_1\,\theta_0) \times$$
$$\frac{\boldsymbol{l}_1\cdot\boldsymbol{k}}{k^2\,\mathcal{D}_0} \exp[\mathrm{i}\boldsymbol{l}_1\cdot\boldsymbol{\gamma}_{12}] \, W\left(|\boldsymbol{l}_1 - \mathcal{D}_0\boldsymbol{k}|\,\theta_0\right) \exp[\mathrm{i}\mathcal{D}_0\boldsymbol{k}\cdot\boldsymbol{\gamma}_{23}]$$
$$W\left(|\boldsymbol{l}_2 - \mathcal{D}_0\boldsymbol{k}|\,\theta_0\right) \exp[\mathrm{i}\boldsymbol{l}_2\cdot\boldsymbol{\gamma}_{34}] \frac{\boldsymbol{l}_2\cdot\boldsymbol{k}}{k^2\,\mathcal{D}_0} \, W(l_2\,\theta_0).$$

In the following I will estimate this expression for different hypothesis on $\boldsymbol{\gamma}_1$, $\boldsymbol{\gamma}_2$, $\boldsymbol{\gamma}_3$ and $\boldsymbol{\gamma}_4$.

A.1 Four separate Directions

Here I assume that

$$\theta_0 \ll \boldsymbol{\gamma}_{ij} \quad \text{whatever } i \text{ and } j. \tag{43}$$

The integral (42) will be dominated by values of l_1, l_2 and k for which $l_1\,\boldsymbol{\gamma}_{12}$, $l_2\,\boldsymbol{\gamma}_{34}$ and $k\,\boldsymbol{\gamma}_{23}$ are about unity. It implies that $l_i\,\theta_0$ and $|\boldsymbol{l}_i - \mathcal{D}_0\boldsymbol{k}|\,\theta_0$ are all small quantities thus making the filtering effects negligible, so that,

$$C_4(\boldsymbol{\gamma}_1, \boldsymbol{\gamma}_2, \boldsymbol{\gamma}_3, \boldsymbol{\gamma}_4) \approx \int \frac{\mathrm{d}^2\boldsymbol{l}_1}{(2\pi)^2} \, C_{l_1} \int \frac{\mathrm{d}^2\boldsymbol{l}_2}{(2\pi)^2} \, C_{l_2} \times \tag{44}$$
$$\int \mathrm{d}\chi \, w^2(\chi) \int \frac{\mathrm{d}^2\boldsymbol{k}}{(2\pi)^2} \, P(k) \times$$
$$\frac{\boldsymbol{l}_1\cdot\boldsymbol{k}}{k^2\,\mathcal{D}_0} \exp[\mathrm{i}\boldsymbol{l}_1\cdot\boldsymbol{\gamma}_{12} + \mathrm{i}\mathcal{D}_0\boldsymbol{k}\cdot\boldsymbol{\gamma}_{23} + \mathrm{i}\boldsymbol{l}_2\cdot\boldsymbol{\gamma}_{34}] \frac{\boldsymbol{l}_2\cdot\boldsymbol{k}}{k^2\,\mathcal{D}_0}.$$

An interesting property to be used is that

$$\int \frac{\mathrm{d}^2 \boldsymbol{l}}{(2\pi)^2} C_l \, \exp[\mathrm{i}\boldsymbol{l} \cdot \boldsymbol{\gamma}] \frac{\boldsymbol{l} \cdot \boldsymbol{x}}{l\, x} = -\frac{\boldsymbol{\gamma} \cdot \boldsymbol{x}}{\gamma\, x} \int \frac{l \mathrm{d}l}{2\pi} C_l \, J_1(l\, \boldsymbol{\gamma}). \quad (45)$$

It implies that

$$C_4(\boldsymbol{\gamma}_1, \boldsymbol{\gamma}_2, \boldsymbol{\gamma}_3, \boldsymbol{\gamma}_4) = \quad (46)$$
$$\frac{\mathrm{d}C(\boldsymbol{\gamma})}{\mathrm{d}\boldsymbol{\gamma}}(\boldsymbol{\gamma}_{12}) \frac{\mathrm{d}C(\boldsymbol{\gamma})}{\mathrm{d}\boldsymbol{\gamma}}(\boldsymbol{\gamma}_{34}) \int \mathrm{d}\chi \, w^2(\chi) \times$$
$$\int \frac{\mathrm{d}^2 \boldsymbol{k}}{(2\pi)^2} \frac{P(k)}{k^2 \, \mathcal{D}_0^2} \frac{\boldsymbol{\gamma}_{12} \cdot \boldsymbol{k}}{\gamma_{12}\, k} \frac{\boldsymbol{\gamma}_{34} \cdot \boldsymbol{k}}{\gamma_{34}\, k} \, \exp[\mathrm{i}\mathcal{D}_0 \boldsymbol{k} \cdot \boldsymbol{\gamma}_{23}],$$

with,

$$C(\boldsymbol{\gamma}) = \int \frac{\mathrm{d}^2 \boldsymbol{l}}{(2\pi)^2} C_l \, e^{\mathrm{i}\boldsymbol{l}\cdot\boldsymbol{\gamma}}. \quad (47)$$

This integral can be eventually integrated from properties of Bessel functions,

$$\int_0^{2\pi} \mathrm{d}\phi \, \exp[\mathrm{i}x\cos(\phi)] \, \cos^2(\phi) = \pi \, [J_0(x) - J_2(x)], \quad (48)$$

$$\int_0^{2\pi} \mathrm{d}\phi \, \exp[\mathrm{i}x\cos(\phi)] \, \sin^2(\phi) = \pi \, [J_0(x) + J_2(x)], \quad (49)$$

$$\int_0^{2\pi} \mathrm{d}\phi \, \exp[\mathrm{i}x\cos(\phi)] \, \sin(\phi) \, \cos(\phi) = 0, \quad (50)$$

with which we find,

$$\left\langle \delta_T^{\mathrm{obs.}}(\boldsymbol{\gamma}_1) \, \delta_T^{\mathrm{obs.}}(\boldsymbol{\gamma}_2) \, \delta_T^{\mathrm{obs.}}(\boldsymbol{\gamma}_3) \, \delta_T^{\mathrm{obs.}}(\boldsymbol{\gamma}_4) \right\rangle_c = \quad (51)$$
$$\frac{1}{2} \frac{\mathrm{d}}{\mathrm{d}\boldsymbol{\gamma}} C(\boldsymbol{\gamma}_{12}) \frac{\mathrm{d}}{\mathrm{d}\boldsymbol{\gamma}} C(\boldsymbol{\gamma}_{34}) \times$$
$$[D_0(\boldsymbol{\gamma}_{23}) \cos(\varphi_{12} - \varphi_{34}) - D_2(\boldsymbol{\gamma}_{23}) \cos(\varphi_{12} + \varphi_{34})],$$

where,

$$D_p(\boldsymbol{\gamma}) = \int \mathrm{d}\chi \, w^2(\chi) \int \frac{k\,\mathrm{d}k}{2\pi} \frac{P(k)}{k^2} \, J_p(\mathcal{D}_0\, k\, \boldsymbol{\gamma}), \quad (52)$$

φ_{12} is the angle between $\boldsymbol{\gamma}_{12}$ and $\boldsymbol{\gamma}_{23}$ and φ_{34} is the angle between $\boldsymbol{\gamma}_{43}$ and $\boldsymbol{\gamma}_{32}$ (see Fig. 1).

A.2 When two Directions Coincide

A.2.a When $\boldsymbol{\gamma}_1 = \boldsymbol{\gamma}_2$

In this case, l_1 is expected to be of the order of $1/\theta_0$, thus larger than k so that

$$W\left(|\boldsymbol{l}_1 - \mathcal{D}_0 \boldsymbol{k}|\, \theta_0\right) \approx W(l_1\, \theta_0) - \quad (53)$$
$$\frac{\boldsymbol{l}_1 \cdot \boldsymbol{k}}{l_1} \theta_0 \, \mathcal{D}_0 \, W'(l_1\, \theta_0) + \dots$$

As a result one has,

$$C_4(\boldsymbol{\gamma}_1, \boldsymbol{\gamma}_1, \boldsymbol{\gamma}_2, \boldsymbol{\gamma}_3) = \int \frac{\mathrm{d}^2 \boldsymbol{l}_1}{(2\pi)^2} C_{l_1} \int \frac{\mathrm{d}^2 \boldsymbol{l}_2}{(2\pi)^2} C_{l_2} \quad (54)$$

$$\int \mathrm{d}\chi \, w^2(\chi) \int \frac{\mathrm{d}^2 \boldsymbol{k}}{(2\pi)^2} P(k) \times$$
$$\exp[\mathrm{i}\mathcal{D}_0 \boldsymbol{k} \cdot \boldsymbol{\gamma}_{12} + \mathrm{i}\boldsymbol{l}_2 \cdot \boldsymbol{\gamma}_{23}] \frac{\boldsymbol{l}_2 \cdot \boldsymbol{k}}{k^2 \, \mathcal{D}_0} \times$$
$$\left(W^2(l_1\,\theta_0) \frac{\boldsymbol{l}_1 \cdot \boldsymbol{k}}{k^2 \, \mathcal{D}_0} - \theta_0 \, W'(l_1\,\theta_0)\, W(l_1\,\theta_0) \frac{(\boldsymbol{l}_1 \cdot \boldsymbol{k})^2}{l_1\, k^2} \right).$$

When one integrates over the angle of $\boldsymbol{l}_1$ the first term vanishes. The second term of the expansion is thus the dominant contribution, which takes the form,

$$C_4(\boldsymbol{\gamma}_1, \boldsymbol{\gamma}_1, \boldsymbol{\gamma}_2, \boldsymbol{\gamma}_3) = -\frac{1}{4} \theta_0 \frac{\mathrm{d}\overline{C}(\theta_0)}{\mathrm{d}\theta} \int \frac{\mathrm{d}^2 \boldsymbol{l}_2}{(2\pi)^2} C_{l_2} \quad (55)$$
$$\int \mathrm{d}\chi \, w^2(\chi) \int \frac{\mathrm{d}^2 \boldsymbol{k}}{(2\pi)^2} P(k) \times$$
$$\exp[\mathrm{i}\mathcal{D}_0 \boldsymbol{k} \cdot \boldsymbol{\gamma}_{12} + \mathrm{i}\boldsymbol{l}_2 \cdot \boldsymbol{\gamma}_{23}] \frac{\boldsymbol{l}_2 \cdot \boldsymbol{k}}{k^2}.$$

Using the property (45) we have

$$C_4(\boldsymbol{\gamma}_1, \boldsymbol{\gamma}_1, \boldsymbol{\gamma}_2, \boldsymbol{\gamma}_3) = -\frac{1}{4} \theta_0 \frac{\mathrm{d}\overline{C}(\theta_0)}{\mathrm{d}\theta} \frac{\mathrm{d}}{\mathrm{d}\boldsymbol{\gamma}} C(\boldsymbol{\gamma}_{23}) \times \quad (56)$$
$$\frac{\boldsymbol{\gamma}_{12} \cdot \boldsymbol{\gamma}_{23}}{\gamma_{23}} \int \mathrm{d}\chi \, w^2(\chi) \times$$
$$\int \frac{k\,\mathrm{d}k}{2\pi} P(k) \frac{J_0(\mathcal{D}_0\, k\, \gamma_{12}) + J_2(\mathcal{D}_0\, k\, \gamma_{12})}{2}.$$

Interestingly C_4 is now proportional to the angular correlation function of the local *magnification* and not of the local displacement.

A.2.b When $\boldsymbol{\gamma}_2 = \boldsymbol{\gamma}_3$

In this case k is expected to be of the order of $1/\theta_0$, thus larger than l_1 and l_2. As a result one has,

$$C_4(\boldsymbol{\gamma}_1, \boldsymbol{\gamma}_2, \boldsymbol{\gamma}_2, \boldsymbol{\gamma}_3) = \int \frac{\mathrm{d}^2 \boldsymbol{l}_1}{(2\pi)^2} C_{l_1} \int \frac{\mathrm{d}^2 \boldsymbol{l}_2}{(2\pi)^2} C_{l_2} \quad (57)$$
$$\int \mathrm{d}\chi \, w^2(\chi) \int \frac{\mathrm{d}^2 \boldsymbol{k}}{(2\pi)^2} P(k) \times$$
$$\exp[\mathrm{i}\boldsymbol{l}_1 \cdot \boldsymbol{\gamma}_{12} + \mathrm{i}\boldsymbol{l}_2 \cdot \boldsymbol{\gamma}_{23}] \frac{\boldsymbol{l}_2 \cdot \boldsymbol{k}}{k^2 \, \mathcal{D}_0} W^2(k\,\theta_0) \frac{\boldsymbol{l}_1 \cdot \boldsymbol{k}}{k^2 \, \mathcal{D}_0},$$

leading to

$$C_4(\boldsymbol{\gamma}_1, \boldsymbol{\gamma}_2, \boldsymbol{\gamma}_2, \boldsymbol{\gamma}_3) = \frac{1}{2} \frac{\mathrm{d}}{\mathrm{d}\boldsymbol{\gamma}} C(\boldsymbol{\gamma}_{12}) \frac{\mathrm{d}}{\mathrm{d}\boldsymbol{\gamma}} C(\boldsymbol{\gamma}_{23}) \times \quad (58)$$
$$\cos(\psi)\, \overline{D}_0(\theta_0),$$

where

$$\overline{D}_0(\theta) = \int \mathrm{d}\chi \, w^2(\chi) \int \frac{k\,\mathrm{d}k}{2\pi} \frac{P(k)}{k^2 \, \mathcal{D}_0^2} \, W^2(\mathcal{D}_0\, k\, \theta). \quad (59)$$

Here the effect is proportional to the mean displacement in the beam size θ_0.

A.2.c Other Cases

The other cases do not give specific formulae and can be derived from results of section A.1.

A.3 When two Pairs Coincide

A.3.a When $\boldsymbol{\gamma}_1 = \boldsymbol{\gamma}_2$ and $\boldsymbol{\gamma}_3 = \boldsymbol{\gamma}_4$

This case is similar to the A.2.b case where the result is dominated by the second order term of an expansion in $k\,\theta_0$, that here should be written for $\boldsymbol{l}_1$ and $\boldsymbol{l}_2$. We then have

$$C_4(\boldsymbol{\gamma}_1, \boldsymbol{\gamma}_1, \boldsymbol{\gamma}_2, \boldsymbol{\gamma}_2) = \int \frac{\mathrm{d}^2\boldsymbol{l}_1}{(2\pi)^2}\, C_{l_1} \int \frac{\mathrm{d}^2\boldsymbol{l}_2}{(2\pi)^2}\, C_{l_2}$$

$$\int \mathrm{d}\chi\, w^2(\chi) \int \frac{\mathrm{d}^2\boldsymbol{k}}{(2\pi)^2}\, P(k) \times \tag{60}$$

$$l_1\theta_0\, W(l_1\,\theta_0)\, W'(l_1\,\theta_0) \left(\frac{\boldsymbol{l}_1 \cdot \boldsymbol{k}}{k\, l_1}\right)^2 \exp[\mathrm{i}\mathcal{D}_0\boldsymbol{k} \cdot \boldsymbol{\gamma}_{12}] \times$$

$$\left(\frac{\boldsymbol{l}_2 \cdot \boldsymbol{k}}{k\, l_2}\right)^2 l_2\theta_0\, W(l_2\,\theta_0)\, W'(l_2\,\theta_0).$$

The integrations over the angles between $\boldsymbol{l}_1$ and $\boldsymbol{k}$ and between $\boldsymbol{l}_2$ and $\boldsymbol{k}$ give each a factor $1/2$ leading to

$$C_4(\boldsymbol{\gamma}_1, \boldsymbol{\gamma}_1, \boldsymbol{\gamma}_2, \boldsymbol{\gamma}_2) = \frac{1}{16} \left(\theta_0 \frac{\mathrm{d}\overline{C}(\theta_0)}{\mathrm{d}\theta}\right)^2 \times \tag{61}$$

$$\int \mathrm{d}\chi\, w^2(\chi) \int \frac{\mathrm{d}^2\boldsymbol{k}}{(2\pi)^2}\, P(k) \exp[\mathrm{i}\mathcal{D}_0\boldsymbol{k} \cdot \boldsymbol{\gamma}_{12}],$$

which can be expressed in terms of the angular correlation function of the magnification.

A.3.b When $\boldsymbol{\gamma}_1 = \boldsymbol{\gamma}_4$ and $\boldsymbol{\gamma}_2 = \boldsymbol{\gamma}_3$

This case is a particular case of subsection A.2.a.

A.4 When the four Directions Coincide

In this case we have

$$C_4 = \int \frac{\mathrm{d}^2\boldsymbol{l}_1}{(2\pi)^2}\, C_{l_1} \int \frac{\mathrm{d}^2\boldsymbol{l}_2}{(2\pi)^2}\, C_{l_2} \int \mathrm{d}\chi\, w^2(\chi)$$

$$\int \frac{\mathrm{d}^2\boldsymbol{k}}{(2\pi)^2}\, P(k)\, \frac{\boldsymbol{l}_2 \cdot \boldsymbol{k}}{k^2\, \mathcal{D}_0}\, \frac{\boldsymbol{l}_1 \cdot \boldsymbol{k}}{k^2\, \mathcal{D}_0} \times \tag{62}$$

$$W(|\boldsymbol{l}_1 - \mathcal{D}_0\boldsymbol{k}|\,\theta_0)\, W(|\boldsymbol{l}_2 - \mathcal{D}_0\boldsymbol{k}|\,\theta_0)\, W(l_1\,\theta_0)\, W(l_2\,\theta_0).$$

This expression cannot be simplified furthermore if the window function is not specified. In this paragraph I assume that W is the top-hat window function,

$$W(x) = \frac{2\, J_1(x)}{x}. \tag{63}$$

To complete the calculation it is interesting to have in mind the property (Bernardeau 1995),

$$\int \frac{\mathrm{d}^2\boldsymbol{l}_1}{(2\pi)^2}\, \frac{\mathrm{d}^2\boldsymbol{l}_2}{(2\pi)^2}\, W|\boldsymbol{l}_1 + \boldsymbol{l}_2| \left(1 + \frac{\boldsymbol{l}_1 \cdot \boldsymbol{l}_2}{l_1^2}\right) = \tag{64}$$

$$\int \frac{l_1\mathrm{d}l_1}{2\pi}\, W(l_1) \int \frac{l_2\mathrm{d}l_2}{2\pi} \left[W(l_2) + \frac{1}{2}\, l_2\, W'(l_2)\right].$$

This property is rigorously exact. In principle it is not possible to separate the two terms. Both relations are however good approximation as it will be shown in the following. It is thus reasonable to assume that

$$\int \frac{\mathrm{d}^2\boldsymbol{l}_1}{(2\pi)^2}\, \frac{\mathrm{d}^2\boldsymbol{l}_2}{(2\pi)^2}\, W|\boldsymbol{l}_1 + \boldsymbol{l}_2|\, \frac{\boldsymbol{l}_1 \cdot \boldsymbol{l}_2}{l_1^2} \approx \tag{65}$$

$$\frac{1}{2} \int \frac{l_1\mathrm{d}_1^l}{(2\pi)}\, W(l_1) \int \frac{l_2\mathrm{d}l_2}{(2\pi)}\, l_2\, W'(l_2).$$

Then, using this property it is easy to show that

$$C_4 = \frac{1}{16} \left(\frac{\mathrm{d}\log[\overline{C}(\theta_0)]}{\mathrm{d}\log[\theta]}\right)^2 \overline{M}_0(\theta_0). \tag{66}$$

A.5 Validity of the top-hat window function property (65)

To examine the property (65), an interesting property of the Bessel function to use is that (Gradshteyn & Ryzhik, 1980, eq. [8.532.1]),

$$\frac{2\, J_1(|\boldsymbol{k}_1 + \boldsymbol{k}_2|)}{|\boldsymbol{k}_1 + \boldsymbol{k}_2|} = \sum_{p=0}^{\infty} (1 + p)\, \frac{2\, J_1(k_1)}{k_1}\, \frac{2\, J_1(k_2)}{k_2} \times \tag{67}$$

$$C_p^1\left(-\frac{\boldsymbol{k}_1 \cdot \boldsymbol{k}_2}{k_1 k_2}\right),$$

with

$$C_p^1\left[-\cos(\varphi)\right] = (-1)^{p+1}\, \frac{\sin(p+1)\varphi}{\sin(\varphi)}. \tag{68}$$

We have thus

$$\int_0^{2\pi} \mathrm{d}\varphi\, C_p^1(-\cos(\varphi)) = 0 \quad \text{for} \quad p \quad \text{odd}, \tag{69}$$

and

$$\int_0^{2\pi} \mathrm{d}\varphi\, C_p^1(-\cos(\varphi)) = 2\pi \quad \text{for} \quad p \quad \text{even}. \tag{70}$$

As a result

$$C_4 = 2^6 \int \frac{\mathrm{d}l_1}{2\pi}\, C_{l_1} \int \frac{\mathrm{d}k}{2\pi}\, P(k) \int \frac{\mathrm{d}l_2}{2\pi}\, C_{l_2} \tag{71}$$

$$J_1(l_1\,\theta_0)\, J_1(l_2\,\theta_0) \sum_{p_1, p_2} (1 + 2p_1)\,(1 + 2p_2) \times$$

$$J_{1+2p_1}(l_1\,\theta_0)\, J_{1+2p_1}(k\,\theta_0)\, J_{1+2p_2}(k\,\theta_0)\, J_{1+2p_2}(l_2\,\theta_0)$$

In the following I assume a power law behavior for both the mass power spectrum and C_l,

$$P(k) \propto k^{n_w},\qquad(72)$$
$$C_l \propto l^{n_c}.\qquad(73)$$

Then using the property,

$$\int_0^\infty J_\nu(t)\,J_\mu(t)\,t^{-\lambda}\mathrm{d}t =\qquad(74)$$

$$\frac{\Gamma(\lambda)}{2^\lambda}\,\frac{\Gamma\left(\frac{\nu+\mu-\lambda+1}{2}\right)}{\Gamma\left(\frac{\nu+\mu+\lambda+1}{2}\right)\Gamma\left(\frac{-\nu+\mu+\lambda+1}{2}\right)\Gamma\left(\frac{\nu-\mu+\lambda+1}{2}\right)},$$

one can easily compute the few terms of the previous series. It is found to converge very rapidly. The resulting ratio,

$$r(n_c,n_w)=\sum_{p_1,p_2}(1+2p_1)(1+2p_2)\times\qquad(75)$$
$$\frac{S(p_1,1,n_c)\,S(p_1,p_2,n_w)\,S(1,p_2,n_c)}{S(1,1,n_c)^2\,S(1,1,n_w)},$$

with

$$S(p_1,p_2,n)=\frac{\Gamma\left(1+p_1+p_2+n/2\right)}{\Gamma\left(p_2-p_1+1-n/2\right)}\times\qquad(76)$$
$$\frac{1}{\Gamma\left(p_2+p_1+2-n/2\right)\Gamma\left(-p_2+p_1+1-n/2\right)},$$

is plotting in Fig. 11. It shows that the error made by using the approximation is at most of a few percent for the values of n_c and n_w of interest.
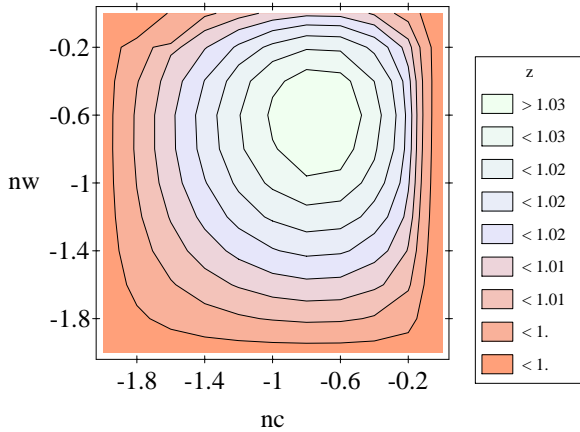

Fig. 11. The ratio (75) as a function of n_c and n_w.